Research Article

Jinlong Xie, Lei Zhu, Hsiao Mun Lee*, and Heow Pueh Lee

Methodologies for the prediction of future aircraft noise level

https://doi.org/10.1515/noise-2024-0005 received February 11, 2024; accepted April 29, 2024

Abstract: This study proposed a method to predict the future aircraft noise level of the international airport by taking Baiyun International Airport (BIA) as an example. BIA was selected to be studied because it is an important international aviation hub in China. The third phase expansion project of BIA is currently in progress, which is the largest airport expansion project in China. The method included the analysis of current operation of the airport, prediction of future operation scenario and operation of the airport, and predicted future population around the airport. Based on the predicted information, this study used CadnaA software to construct and analyze the noise maps of BIA during summer and winter in 2030. The major advancement of this study compared to that of previous research is that this study predicted the noise levels of the airport during summer and winter separately based on the wind direction of airport location, while other research did not take wind direction into consideration. It is found that operation Scenario 1 produces lower noise pollution level in the future compared to Scenario 2 based on the noise exposure results. It is worth mentioning that in 2030 during winter, when the noise level is greater than 70 dB, the noise-exposed area and population of BIA increase by 71.88 and 146.87% (Scenario 1), respectively, compared to current data, which is more serious compared to the growth rate during summer.

Keywords: future aircraft noise, prediction method, CadnaA, pollution, noise control

Jinlong Xie: Department of Mechanical Engineering, National University of Singapore, 9 Engineering Drive 1, Singapore 117575, Singapore, e-mail: jlxie@nus.edu.sg

Lei Zhu: School of Mechanical and Electrical Engineering, Guangzhou University, 230 Wai Huan Xi Road, Guangzhou 510006, P.R. China, e-mail: gzhuzl@outlook.com

Heow Pueh Lee: Department of Mechanical Engineering, National University of Singapore, 9 Engineering Drive 1, Singapore 117575, Singapore, e-mail: mpeleehp@nus.edu.sg

1 Introduction

The global air passenger traffic increased by 70.4% from 2010 to 2019 [1]. With the increment of urbanization in various countries, the global urban population is expected to reach 6 billion people in 2045 (increase about 150% compared to 2020) [2], which will significantly increase people's demand for air travel. However, the increment of air passenger traffic in the future will cause more people's health to be affected by aircraft noise [3], and more airports will face the problem of aircraft noise pollution [4]. Thus, it is very important to predict the future noise level of an airport in order to guide the airport development in a direction that is more beneficial to human health.

Vogiatzis [5] predicted the aircraft noise level of three future scenarios in 2018 based on the historical flight data (2004–2008) of Larnaka International Airport. Thereafter, he optimized the noise action plans of the airport based on the prediction results. Josimović et al. [6] predicted the noise level of Tivat airport in 2030. The results showed that the noise level of Tivat airport would not increase significantly in the future, which provided technical guidance for the future development of the airport. Ozkurt [7] predicted the future noise exposure level of Ankara Esenboğa Airport based on the airport operation data in 2012. The results showed that the noise-exposed population of the airport would increase four times and seven times in 2025 and 2030, respectively. The noise-level prediction data of Imam Khomeini International Airport in 2020 and 2030 from Sadr et al. [8] showed that the joint development of the airport and residential areas would aggravate the aircraft noise pollution. Wolfe et al. [9] compared the future noise levels of Heathrow Airport and Gatwick Airport in 2030. The results showed that the expansion of the two airports in the future would aggravate the impact of aircraft noise on residents and the noise pollution level at Heathrow Airport would be more serious.

The research outcomes of these reported studies provide valuable suggestions for airport decision makers in formulating airport development planning. Therefore, it is

^{*} Corresponding author: Hsiao Mun Lee, Department of Mechanical Engineering, National University of Singapore, 9 Engineering Drive 1, Singapore 117575, Singapore, e-mail: hmlee@nus.edu.sg

valuable to predict future noise level of the airport. In 2020, under the influence of coronavirus disease 2019, the annual passenger throughout Baiyun International Airport (BIA) reached 44 million and ranked first in the world despite the sudden drop in global flight volume based on 2020 Guangzhou traffic development report [10]. Thus, BIA was selected as the study case in the present work due to its high flight volume compared to other airports. In the previous study [11], we already constructed the noise maps of BIA during summer and winter. However, as the passenger traffic of BIA increases from year to year, its current three runways will not be able to sustain higher passenger traffic in the future. In 2019, the annual passenger traffic of BIA was about 73.38 million people, which was close to the maximum designed capacity (80 million people per year) [12]. Thus, in order to sustain the greater demand of passenger traffic, the third phase expansion project of BIA was officially launched in 2020 [13]. This expansion will add two runways and one terminal for BIA in order to meet the passenger traffic demand of 120 million passengers per year in the future [14]. Therefore, the main objective of the current effort is to use CadnaA software to predict the aircraft noise level of BIA in 2030 after the expansion in order to evaluate the future acoustic environment quality of BIA.

2 Methodologies

A low-cost aircraft noise-level prediction method was proposed in this study based on the flight data and details of the airport expansion project. The technical route of the method is shown in Figure 1. This route is applicable to other airports. For example, other airports can first summarize their current operation based on the method proposed in Section 2.1 (aircraft takeoff/landing track, *etc.*). Then, the population around other airports can be estimated using the same strategy proposed in Section 2.6 (United Nations). Consequently, the

future aircraft noise level can be predicted by following all the steps that are listed in Section 2.

2.1 Current operation of BIA

Current operation of BIA was summarized based on the 2-week flight data (summer: 2021 March 25–March 31, winter: 2020 December 14–December 20) that are closest to the annual operation condition of BIA. Please refer to Section 2.13 in Xie *et al.* [11] for more details of the flight data. Current number and proportion of flights under different aircraft tracks at BIA are shown in Table 1. Current operation of BIA during summer and winter is shown in Figures 2 and 3, respectively. The proportions of takeoff and landing flights at BIA are about 51 and 49%, respectively, for both summer and winter (Table 1).

In addition, the aircraft takeoff tracks of BIA are regular where BIA will select the runway and takeoff track based on the relative position between the destination and the airport, as shown in Figures 2 and 3. For example, during summer, the aircrafts generally fly to the cities in the east, southeast, and northeast of BIA using T-20R-A. The aircraft generally fly to the cities in the south and southwest of BIA using T-20R-B and T-19-C. Current aircraft takeoff tracks and the corresponding destinations in BIA during summer and winter are shown in Tables A1 and A2, respectively. There is no regular rule for the landing tracks of BIA, and the proportion of the number of flights on the tracks of the two landing runways is close to 1:1.

2.2 Air traffic volume of BIA in 2030

On 2020 August 25, "Feasibility Study Report on Phase III Expansion Project of Guangzhou Baiyun International Airport" [14] issued by the China Airport Planning & Design Institute Co.,

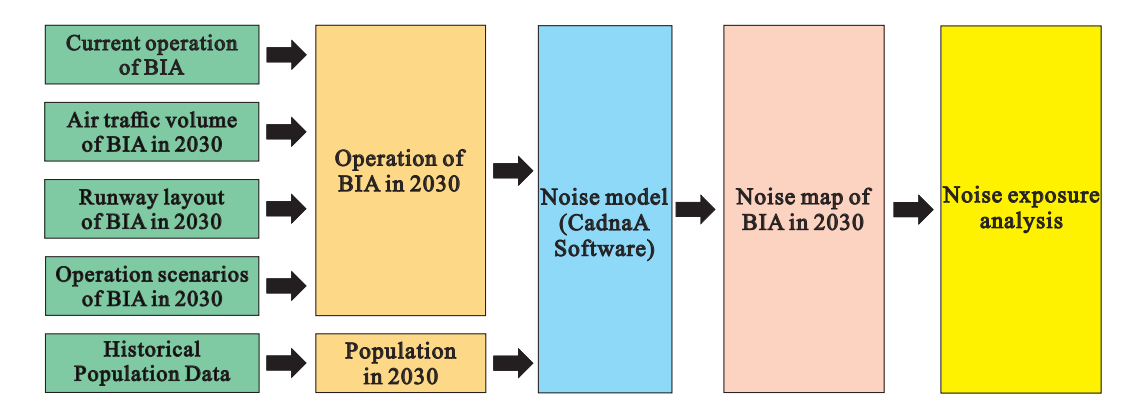


Figure 1: Technical route for predicting aircraft noise level of BIA in 2030.

Table 1: Number and proportion of flights under current aircraft tracks at BIA

Tracks	Number	Proportion (%)	$Track_w$	Number	Proportion (%)
T-19-A	207	17.1	T-01-A	82	6.8
T-19-B	61	5.0	T-01-B	101	8.3
T-19-C	22	1.8	T-01-C	32	2.6
T-20R-A	256	21.2	T-02L-A	11	0.9
T-20R-B	59	4.9	T-02L-B	137	11.3
T-20R-C	9	0.7	T-02L-C	257	21.2
L-19-A	284	23.5	L-01-A	156	12.9
L-19-B	12	1.0	L-01-B	131	10.8
L-20L-A	237	19.6	L-02R-A	138	11.4
L-20L-B	63	5.2	L-02R-B	166	13.7
Total	1210	100	Total	1212	100

Track_s and Track_w are the tracks during summer and winter, respectively. The name of the track consists of three parts. For example, T-20R-A means the flight takeoff at Runway 20R with track A. L-20L-A means flight lands at Runway 20L with track B. Please refer to Section 2.3 in Xie et al. [11] for more details of the aircraft tracks.

Ltd. was approved by China National Development and Reform Commission [15]. Thus, the current airport expansion project is being carried out based on the contents of the report. The report predicted that the air traffic volume of BIA in 2030 (775k sorties, with a daily average of 2,123 sorties) based on the historical flight data. Table 2 shows the takeoff and landing sorties of BIA from 2011 to 2019 and in 2030.

2.3 Runway layout of BIA in 2030

The expanded BIA will have five runways and three terminals [14]. In the present study, the expanded five runways were named as 01L/19R, 01R/19L, 02L/20R, 02R/20L, and 03/21 based on the runway numbers of Shanghai Pudong International Airport and Atlanta International Airport

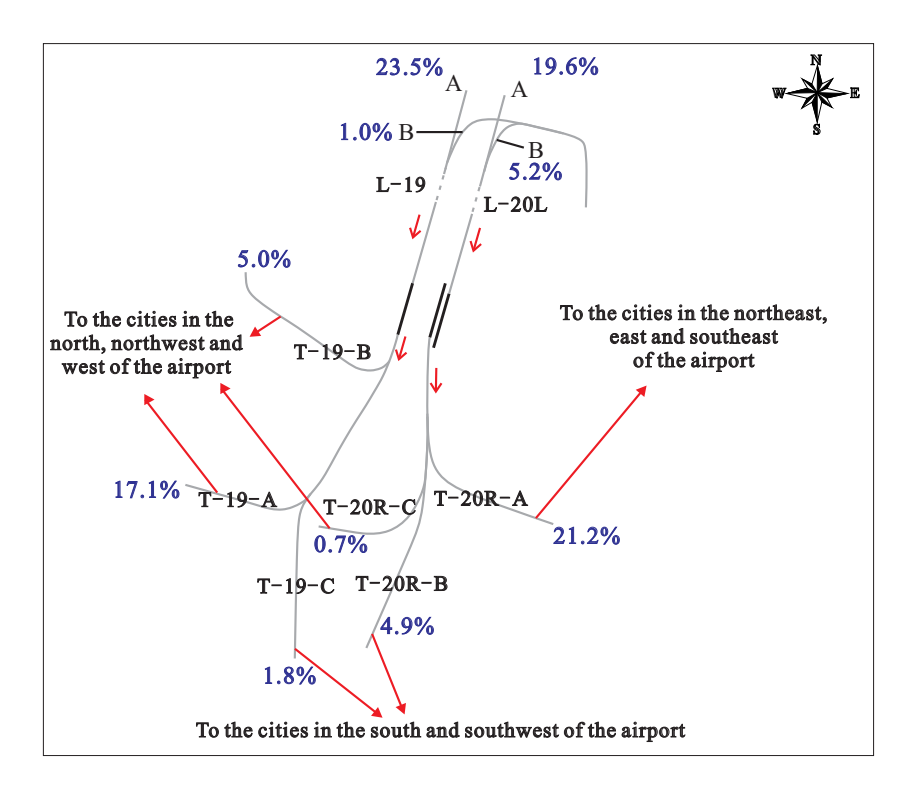


Figure 2: Current operation of BIA during summer (the dotted line is used to omit some straight landing tracks).

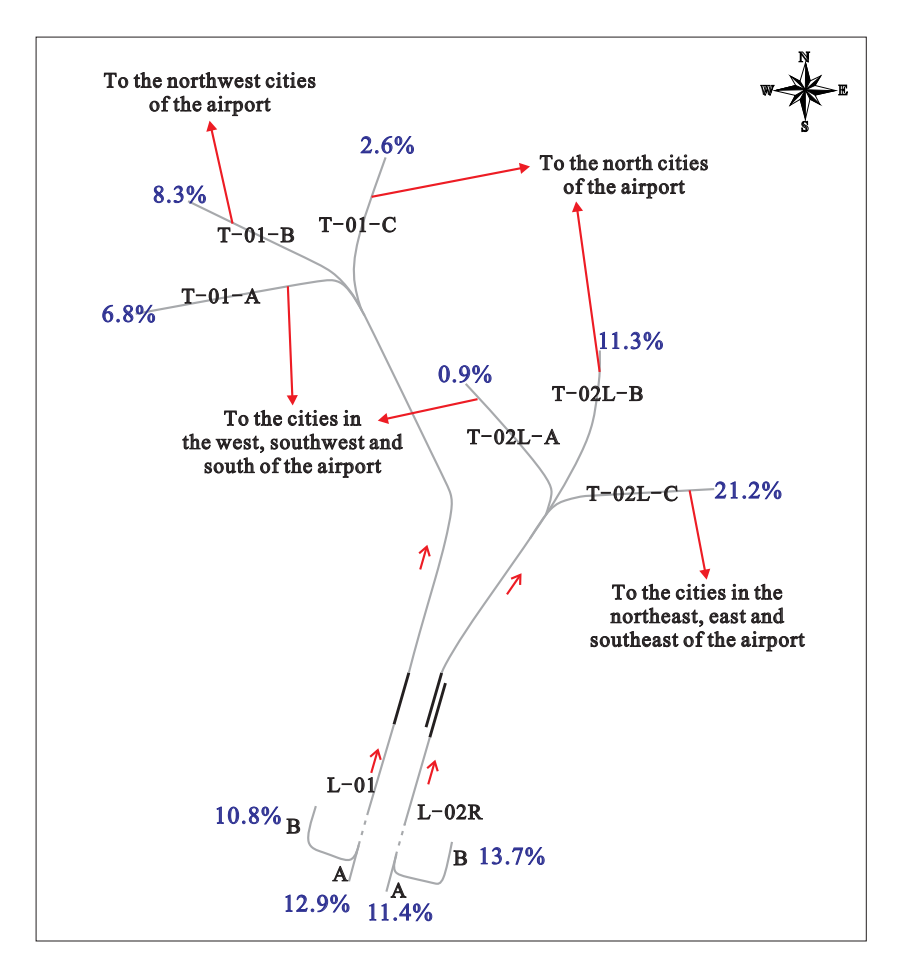


Figure 3: Current operation of BIA during winter (the dotted line is used to omit some straight landing tracks).

where these airports also have five runways. It should be emphasized that the expanded Runways 01R/19L, 02L/20R, and 02R/20L actually are the runways that renamed from the original Runways 01/19, 02L/20R, and 02R/20L (see Figure 2 in Xie *et al.* [11]), respectively. The runway layout of BIA in 2030 is shown in Figure 4.

Table 2: Takeoff and landing sorties of BIA from 2011 to 2019 and in 2030 (*predicted year) [14]

Year	Annual	Daily
2011	349,000	957
2012	373,000	1,022
2013	394,000	1,079
2014	412,000	1,129
2015	410,000	1,122
2016	435,000	1,192
2017	465,000	1,275
2018	477,000	1,308
2019	491,000	1,345
2030*	775,000	2,123

2.4 Prediction of the operation scenarios of BIA in 2030

"Feasibility Study Report on Phase III Expansion Project of Guangzhou Baiyun International Airport" [14] indicated that after the expansion, three runways of BIA will be used for flight takeoff and three runways will be used for flight landing. Therefore, two operation scenarios of BIA in 2030, as shown in Figure 5, were predicted based on the runway spacing after the expansion (Figure 4), the "three takeoff and three landing rule" as mentioned earlier and the rule of "Regulations on Management of Instrument during Simultaneous Operation of Parallel Runways" [16] (Table A3). It should be noted that these two operation scenarios will be used in both summer and winter. However, the takeoff and landing directions of aircraft during summer and winter are different (Figure 5) since the winds during summer and winter are mainly blowing from south and north, respectively. Following are the details of the two scenarios:

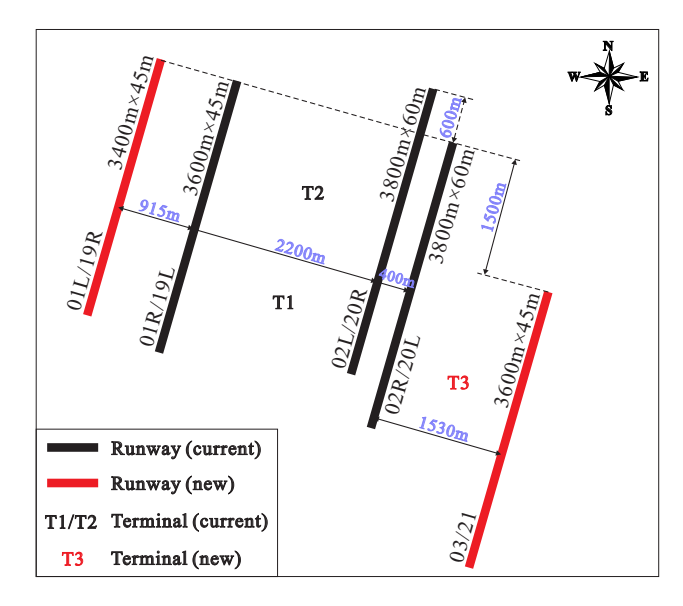


Figure 4: Runway layout after the completion of BIA Phase III expansion project in 2030. It should be take note that, for example, Runway 01L/19R is actually a runway with opposite takeoff and landing directions. It means the takeoff direction of Runway 01L is from south to north and landing direction of Runway 19R is from north to south.

- 1) Scenario 1: Runways 01L/19R and 02R/20L are only used for landing, Runways 02L/20R and 03/21 are only used for takeoff, and Runway 01R/19L is used for both takeoff and landing, as shown in Figure 5(a).
- 2) Scenario 2: Runways 01L/19R and 02R/20L are only used for landing, Runways 02L/20R and 01R/19L are only used for takeoff, and Runway 03/21 is used for both takeoff and landing, as shown in Figure 5(b).

Therefore, the difference between the two scenarios only exists in the landing function of Runways 01R/19L and 03/21, while the operation modes of other runways are the same.

2.5 Prediction of the operation of BIA in 2030

The operation of BIA in 2030 was predicted based on the current operation of BIA (Figures 2 and 3), the predicted operation scenarios of BIA (Figure 5) and the practices of

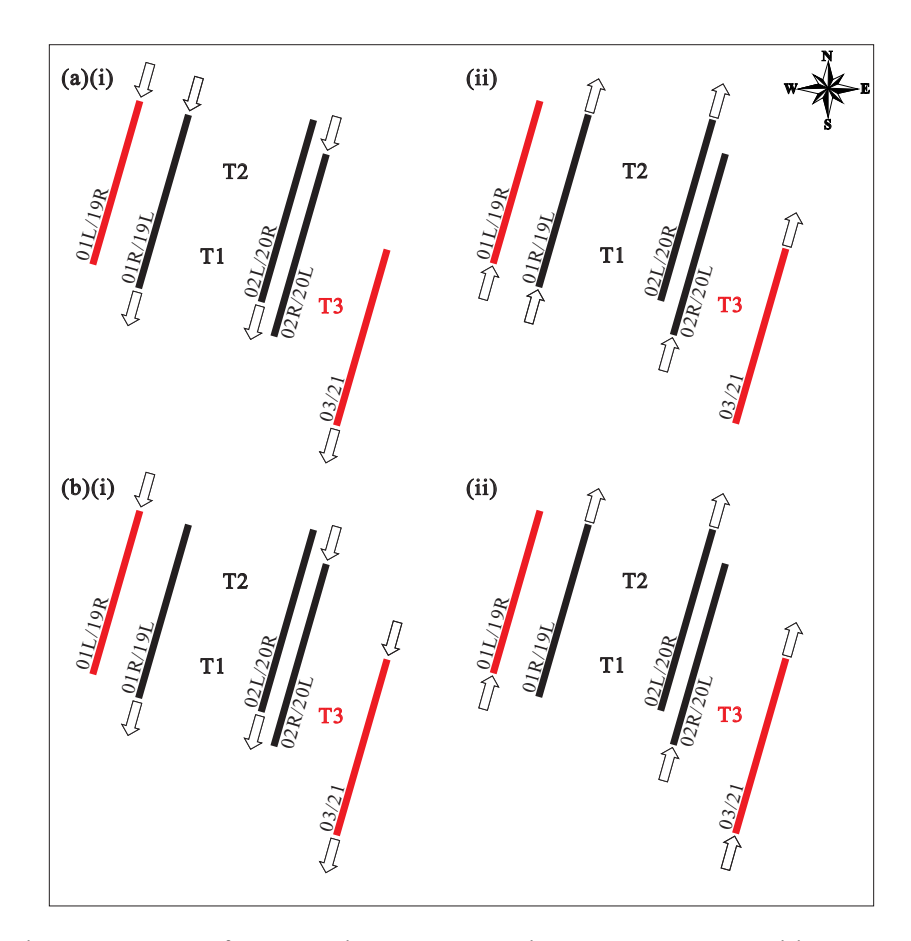


Figure 5: Two predicted operation scenarios of BIA in 2030 during (i) summer and (ii) winter: (a) Scenario 1 and (b) Scenario 2. The arrow pointing to the runway indicates the landing, and the arrow facing away from the runway indicates the takeoff.

Table 3: Number and proportion of flights under future aircraft tracks at BIA in 2030

Track _s	Number	Proportion (%)	$Track_w$	Number	Proportion (%)
T-19L-A	282	13.2	T-01R	361	17.0
T-19L-B	79	3.8	T-02L	361	17.0
T-20R	361	17.0	T-03	361	17.0
T-21	361	17	L-01L	346	16.3
L-19R	346	16.3	L-02R	346	16.3
L-20L	346	16.3	L-01R (S1)	346	16.3
L-19L (S1)	346	16.3	L-03 (S2)	346	16.3
L-21 (S2)	346	16.3			

S1 and S2 are Scenarios 1 and 2, respectively. The name of the track consists of three parts as explained in Table 1. If the runway only has one track (e.g., T-20R), only the first two parts are named. During summer, all tracks are used in both scenarios except L-19L (S1) and L-21 (S2). During winter, all tracks are used in both scenarios except L-01R (S1) and L-03 (S2).

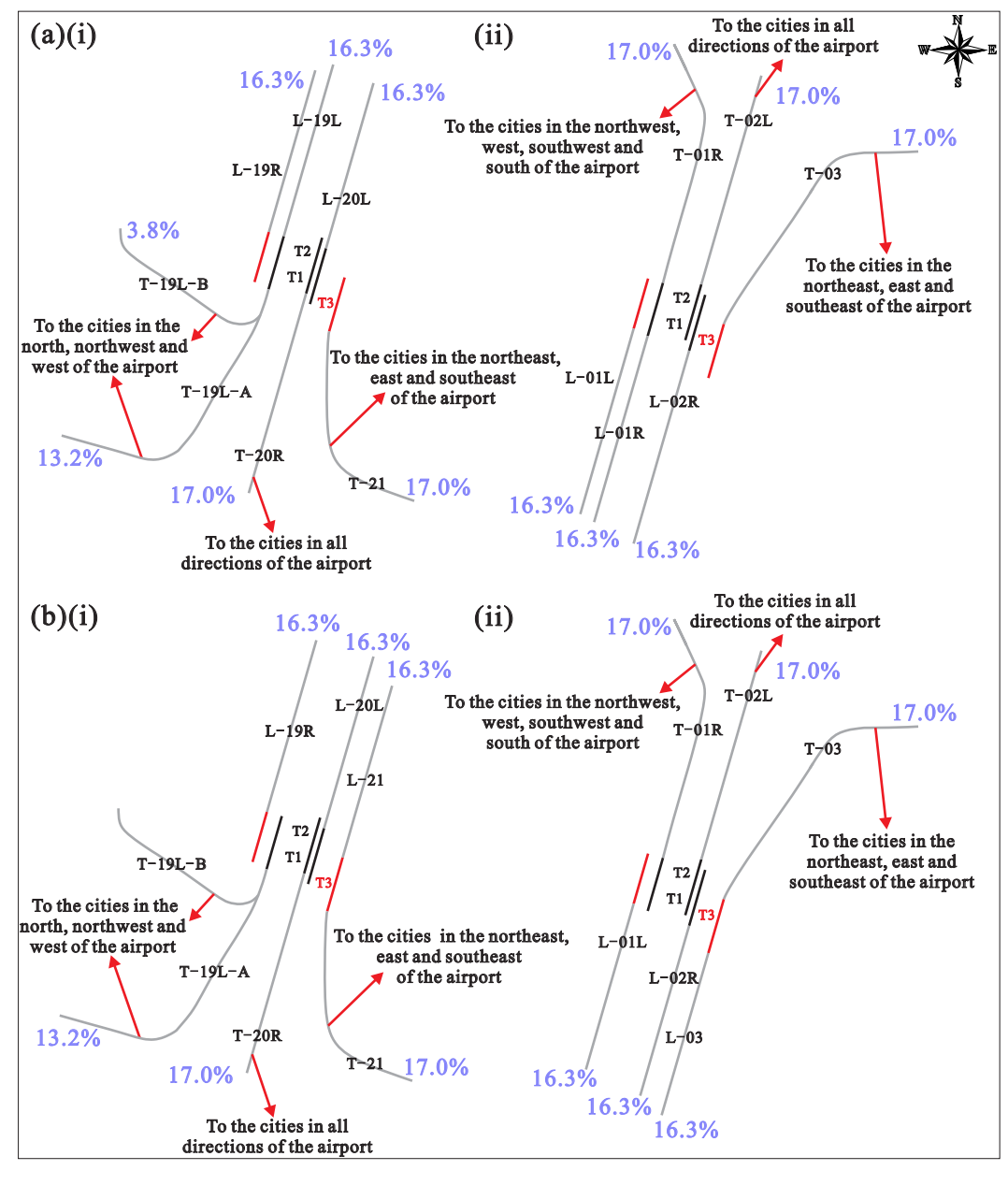


Figure 6: Operation of BIA in 2030 during (i) summer and (ii) winter under Scenarios (a) 1 and (b) 2.



Figure 7: Noise-affected administrative regions around BIA. The blue line indicates the boundary between Huadu District and Baiyun District. The regions in white and yellow fonts belong to Huadu District and Baiyun District, respectively. The administrative regions with * are new added regions after the airport is expanded (see Figure 2 in Xie *et al.* [11] for the noise-affected administrative regions before the airport is expanded).

Table 4: Population of Huadu District and Baiyun District from 2011 to 2020 [18] and in 2030 (*predicted year) [19]

Year **Huadu district Baiyun district** 2011 1,023,500 2,463,900 2,663,000 2012 1,099,600 2013 1,168,700 2,814,300 2014 1,236,000 2,950,400 2015 1,327,000 3,126,500 2016 1,422,400 3,218,500 2017 1,490,700 3,420,100 3,620,000 2018 1,549,200 2019 1,594,500 3,669,500 2020 1,650,900 3,759,100 2030* 2,348,000 5,198,200

other researchers [5,17]. Following are the details of the prediction process:

Table 5: Population of the nine administrative regions around BIA in 2020 [20,21] and 2030 (*predicted year) [19]

District	Region	2020	2030
Huadu	Huadong town	176,063	250,414
	Huashan town	122,929	174,842
	Xinya street	171,899	244,492
Baiyun	Renhe Town	211,248	292,114
	Longgui street	194,776	269,336
	Taihe town	131,793	182,243
	Junhe street	172,155	238,056
	Jiahe street	175,410	242,557
	Zhongluotan town	275,130	380,450

Predict the utilization rate of each runway of BIA in 2030:
 and 49% of the takeoff and landing flights were equally allocated to the three takeoff and three landing

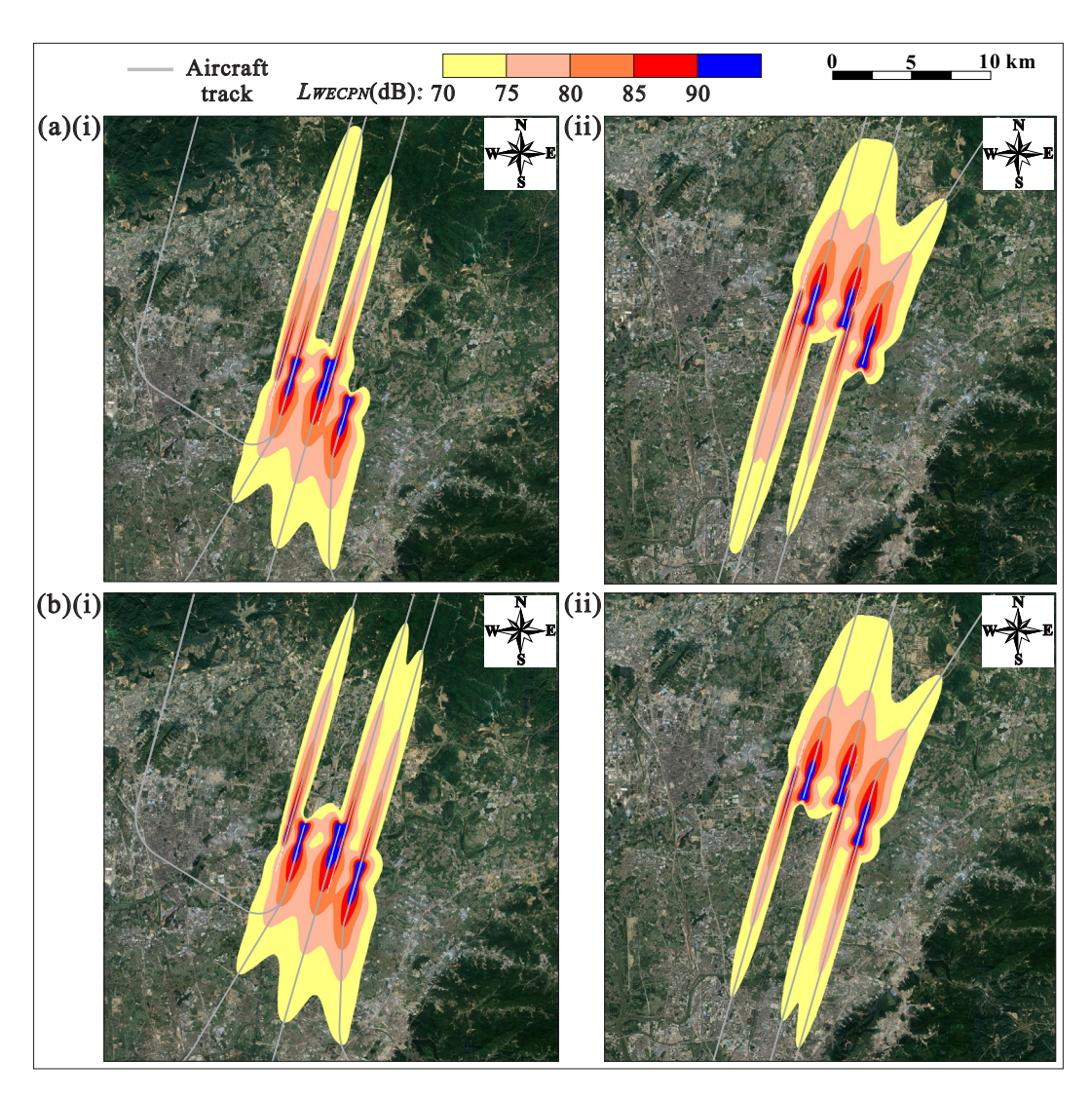


Figure 8: Noise map of BIA in 2030 during (i) summer and (ii) winter under scenarios (a) 1 and (b) 2.

runways after the airport expansion based on the current operation of BIA (Section 2.1), as shown in Table 3.

2) Predict the aircraft track of BIA in 2030 and the proportion of flights per track: in 2030, only one track of each

runway (except Runway 19L) was able to be predicted based on the current track of BIA (Figures 2 and 3), as shown in Figure 6. The ratio of the number of flights on the two tracks of Runway 19L (T-19L-A: 13.2% and T-19L-

Table 6: Noise exposure analysis of BIA in 2030

			$L_{ m WECPN}$ > 70 dB	$L_{ m WECPN}$ > 75 dB	$L_{ m WECPN}$ > 80 dB	$L_{ m WECPN}$ > 85 dB	$L_{ m WECPN}$ > 90 dB
Summer	Scenario 1	Area (km²)	135.848	69.525	30.635	12.413	4.943
		Population	466,843	179,171	26,262	1,893	0
	Scenario 2	Area (km²)	138.165	66.418	30.135	12.295	4.905
		Population	497,153	179,225	25,049	4,196	80
Winter	Scenario 1	Area (km²)	134.730	67.238	28.590	11.670	4.540
		Population	551,167	228,400	60,915	10,998	0
	Scenario 2	Area (km²)	138.198	64.663	28.4	11.633	4.535
		Population	649,545	193,019	46,175	10,374	0

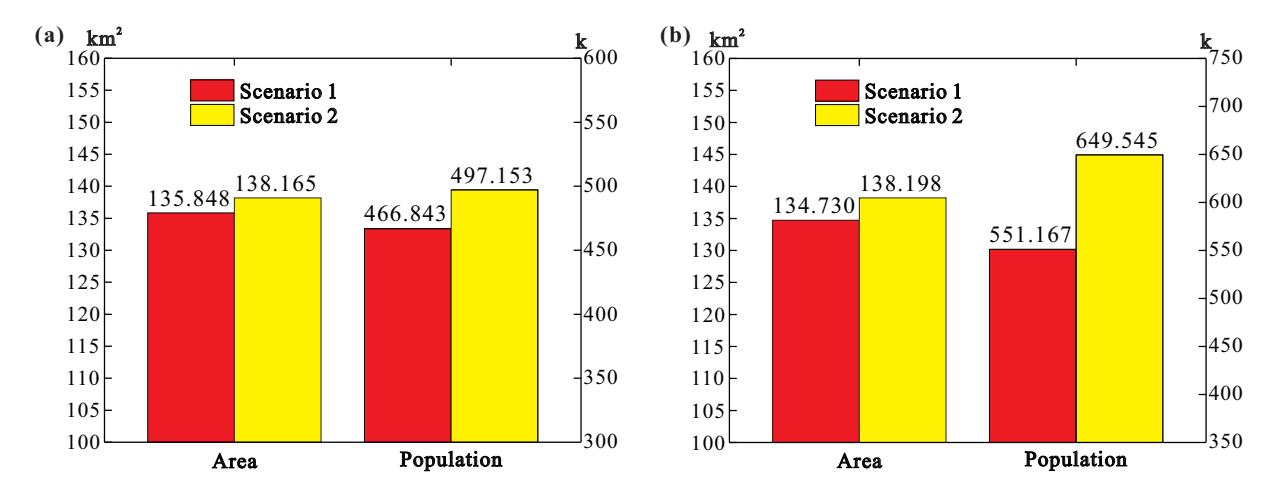


Figure 9: Total area and population of BIA that affected by the noise level (LWECPN) greater than 70 dB in 2030 during (a) summer and (b) winter.

B: 3.8%) was calculated based on the current track and the predicted runway utilization rate, as shown in Figure 6(i). As other runways have only one track, the proportion of flight number of other tracks (takeoff track: 17.0%, landing track is 16.3%) were obtained based on the predicted runway utilization rate, as shown in Figure 6.

- 3) Predict the aircraft track operation of BIA in 2030: the aircraft track operation of BIA in 2030 (Figure 6) was predicted based on the rule of the current track (Figures 2 and 3). Consequently, the takeoff track of BIA in 2030 will operate regularly. For example, during summer (Figure 6(i)), the takeoff track (T-21) of Runway 21 on the east side of BIA is responsible for flights to the cities in the northeast, east, and southeast of the airport. There is no regular rule for the landing tracks of BIA in 2030.
- 4) Proportion of aircraft types of BIA in 2030: the proportion of different aircraft types on each track in 2030 was assumed to be the same with the present proportion.
- 5) Meteorological data of BIA in 2030: the meteorological data (average temperature, humidity, etc.) during summer and winter of 2030 were assumed to be consistent with the current data.

2.6 Prediction of the population around BIA in 2030

BIA is located at the junction of two municipal districts (Huadu District and Baiyun District), as shown in Figure 7. The total population of Huadu District and Baiyun District in recent 10 years (2011-2020) is shown in Table 4 [18]. It is found that the average annual population growths of Huadu District and Baiyun District in recent 10 years are 69,700 peoples and 143,900 peoples, respectively. Population of Huadu District and Baiyun District in 2030 (Table 4) were predicted based on the population data in recent 10 years and the estimation method from United Nations [19].

In this study, four noise-affected administrative regions (totally nine regions) were added based on the preliminary simulation results (compared Figure 7 and Figure 2 in Xie et al. [11]). It is found that that the population growth rates of Huadu District and Baiyun District are 42.23 and 38.28%, respectively, by comparing their predicted population in 2030 and population in 2020 (Table 4). Then, the population of the nine noise-affected administrative regions around BIA in 2030 was calculated based on these grow rates, as shown in Table 5. Finally, population densities of the nine administrative regions in 2030 were calculated as shown in Table A4.

3 Results and discussion

3.1 Comparison between the noise exposure levels of the two operation scenarios

CadnaA software was used to construct noise maps based on the two operation scenarios of BIA in 2030, as shown in Figure 8, using the prediction methodologies and information that are presented in Section 2. The details of the aircraft noise map construction steps can be found in the study of Xie et al. [11]. The data in Table 6 and Figures 9 and 10 were extracted from the noise maps in Figure 8.

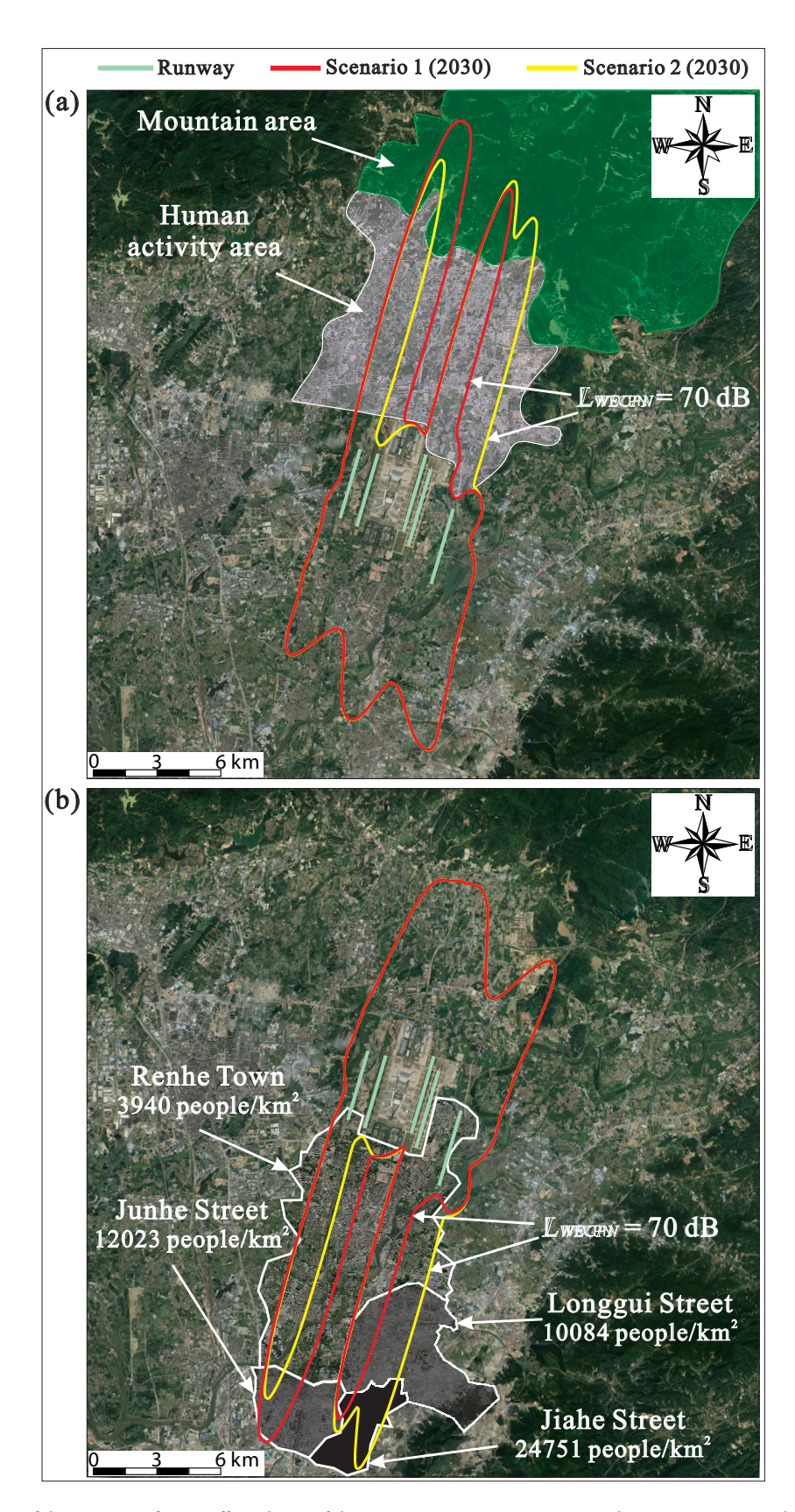


Figure 10: Comparison of the contours of noise-affected area of the two operation scenarios in 2030 during (a) summer and (b) winter (darker color represents the greater population density).

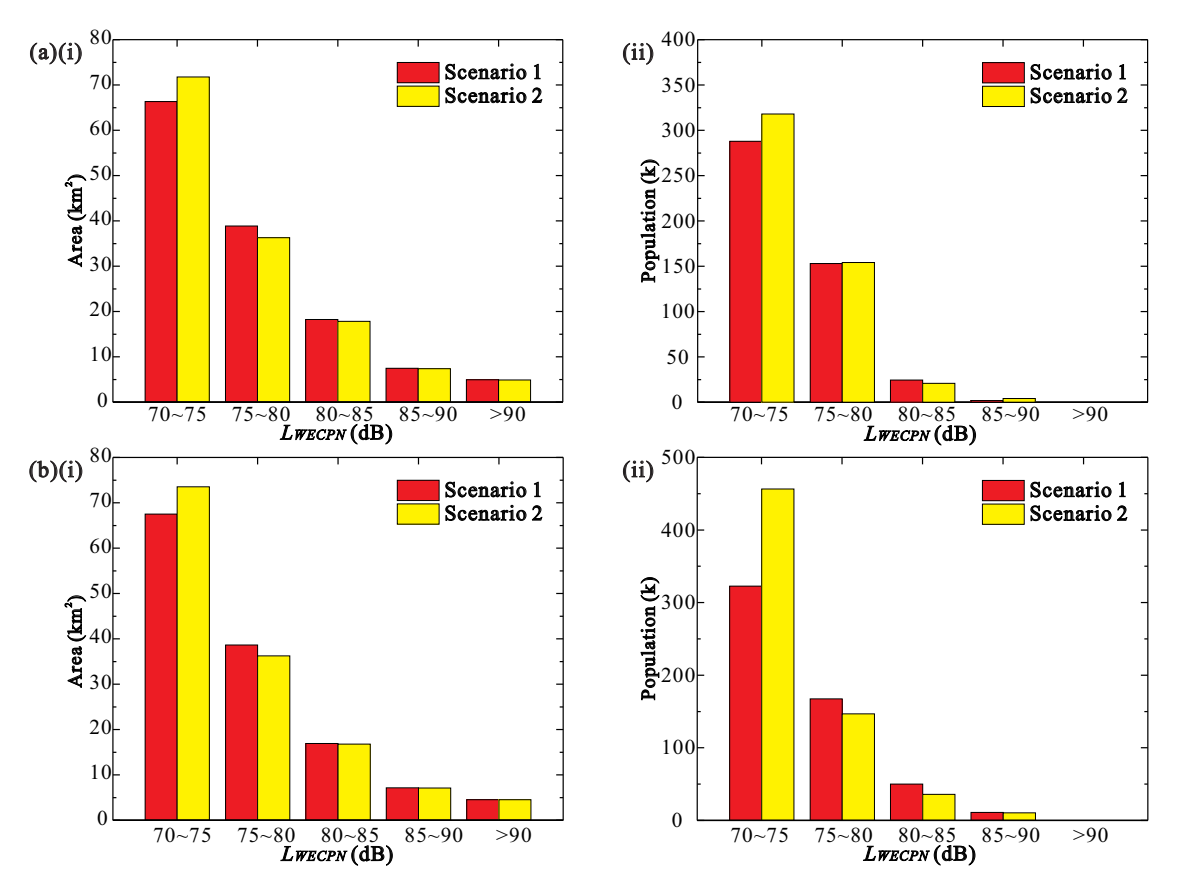


Figure 11: Noise-affected area and population under different ranges of LWECPN in 2030 during (a) summer and (b) winter. (i) Area (ii) population.

During summer, when $L_{\rm WECPN} > 70\,$ dB, it is found that even Scenario 2 only produces 2.317 km² more noise-affected area compare to Scenario 1 as shown in Table 6, but the noise-affected population of Scenario 2 is 30,310 more people than Scenario 1. This is because first, it can be seen from Figure 9(a) that the north longitudinal extension range of the noise contour (red) of Scenario 1 is significantly larger than that of Scenario 2 (yellow). Consequently, Scenario 1 covers more mountain areas compared to Scenario 2. Second, the north horizontal extension range of the noise contour of Scenario 2 is significantly larger than that of Scenario 1. Consequently, Scenario 2 covers more human activity areas compared to Scenario 1.

During winter, when $L_{\rm WECPN} > 70$ dB, the noise-affected area of Scenario 2 is also slightly higher than that of Scenario 1 (3.468 km² more), but the noise-affected population is 98,378 more people than that of Scenario 1 (Table 6). This is because during winter, the south noise contour of Scenario 1 extends southward, covers the main area of Renhe Town (3,940 people/km²) and Junhe street (12,023 people/km²), as shown in Figure 10(b). The south noise contour of Scenario 2 covers Longgui street (10,084 people/km²) and Jiahe street (2,4751 people/km²) with greater population

density. In addition, Figure 11 shows that the differences between the noise-affected area and population caused by the two scenarios are mainly occur in the range of 70 dB $< L_{\rm WECPN} <$ 75 dB, while there is no significant difference in other ranges of $L_{\rm WECPN}$. Therefore, it is recommended that BIA selects Scenario 1 as its operation scenario in 2030 since Scenario 1 produces lesser noise-affected areas and population during both summer and winter.

3.2 Comparison between the current and future noise exposure levels of BIA

Current noise exposure level of BIA was compared with its future noise exposure level in 2030 using Scenario 1 since the noise pollution degree of Scenario 1 is lower than Scenario 2 as discussed in Section 3.1. Figure 12(a) shows that during summer, the noise-affected area ($L_{\rm WECPN} \geq 70$ dB) of BIA in 2030 increase significantly, which is about 51.963 km² (61.96%) (Table 7). Consequently, the noise-affected population also increases about 272,001 people, which is about 139.60%. During winter (Figure 12(b)), the noise-affected area and

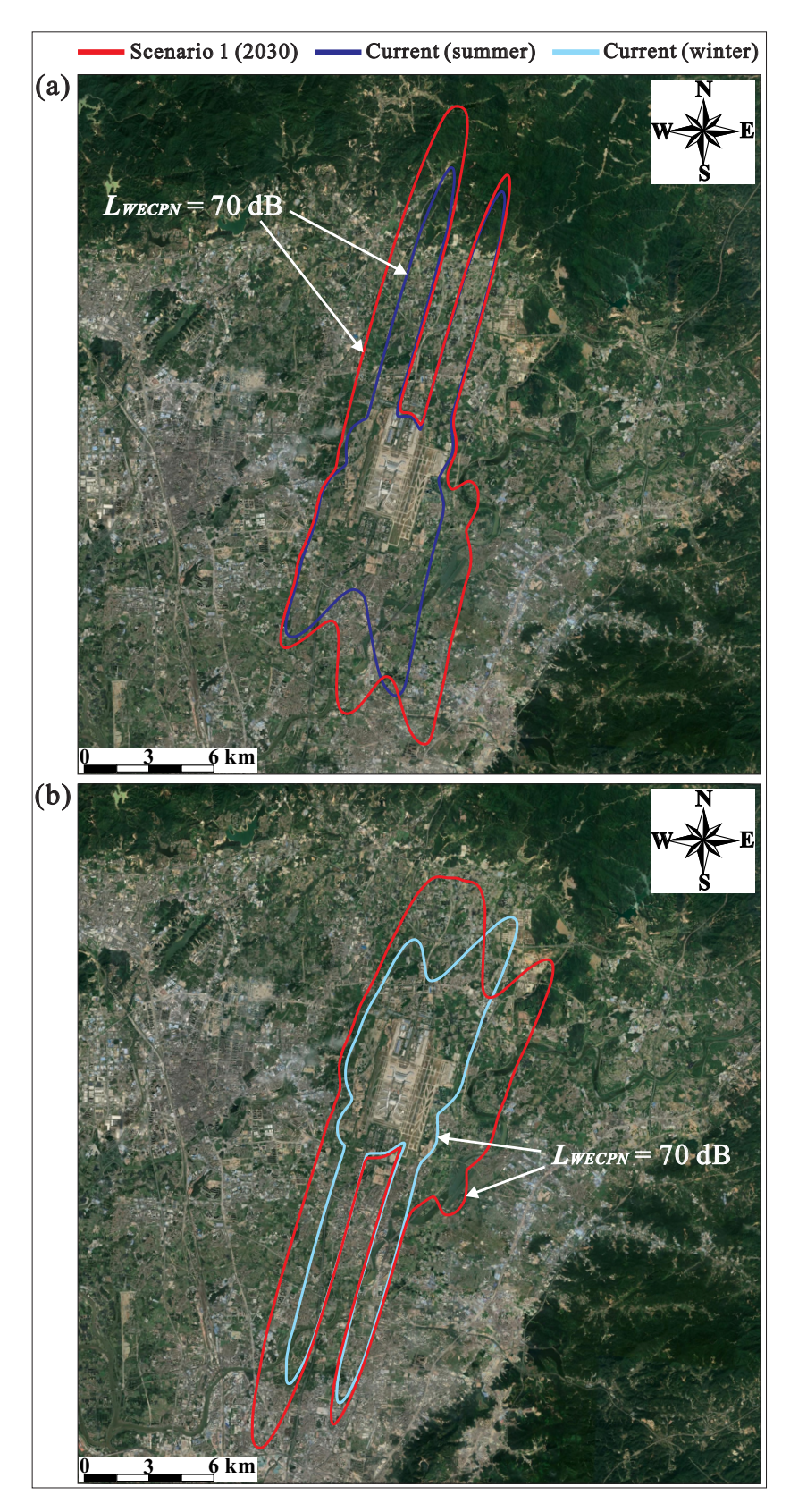


Figure 12: Current and future (2030, Scenario 1) noise contour comparison during (a) summer and (b) winter.

Table 7: Comparison between the current and future (2030, Scenario 1) noise exposure levels of BIA

			$L_{\text{WECPN}} > 70 \text{ dB}$	$L_{\text{WECPN}} > 75 \text{ dB}$	$L_{\text{WECPN}} > 80 \text{ dB}$	$L_{\text{WECPN}} > 85 \text{ dB}$	$L_{\rm WECPN} > 90 \mathrm{dB}$
Summer	Area (km²)	Current	83.885	38.813	16.925	7.165	2.960
		2030	135.848	69.525	30.635	12.413	4.943
		Growth rate (%)	61.95	79.13	81	73.24	66.99
	Population	Current	194,842	75,514	13,414	1,831	155
		2030	466,843	179,171	26,262	1,893	0
		Growth rate (%)	139.60	137.27	95.78	3.39	100
Winter	Area (km²)	Current	78.386	36.249	15.790	6.536	2.594
		2030	134.73	67.238	28.59	11.67	4.54
		Growth rate (%)	71.88	85.49	81.06	78.55	75.02
	Population	Current	223,261	76,473	2,226	4,033	436
		2030	551,167	228,400	60,915	10,998	0
		Growth rate (%)	146.87	198.67	173.65	172.70	-100

population of BIA in 2030 also increase significantly, which are about 56.344 km² (71.88%) and 327,906 people (146.87%), as shown in Table 7. Thus, the noise pollution degree of BIA during winter is more serious than that during summer. It is interesting to take note that the noise-affected area and population under all ranges of $L_{\rm WECPN}$ also increase significantly in

2030 except for the range of $L_{WECPN} > 90$ dB (Table 7 and Figure 13). This is because the expansion of the airport has led to the relocation of residents around the five runways, so no residents are exposed to the area with $L_{\rm WECPN} > 90$ dB. Figure 14 shows that in 2030, the noise-affected area of BIA during winter is 1.118 km² lesser than that during summer.

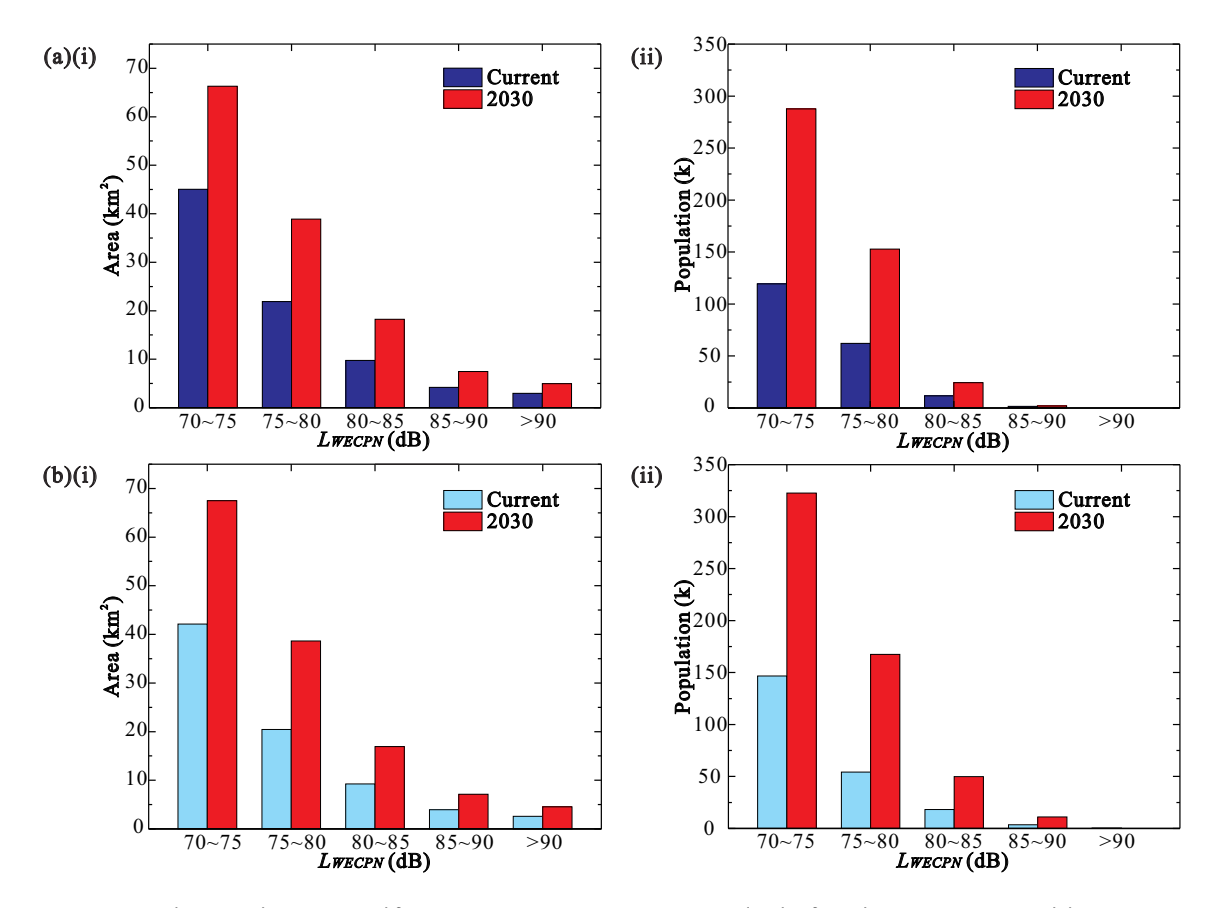


Figure 13: Comparison between the current and future (2030, Scenario 1) noise exposure levels of BIA during (a) summer and (b) winter: (i) area and (ii) population.

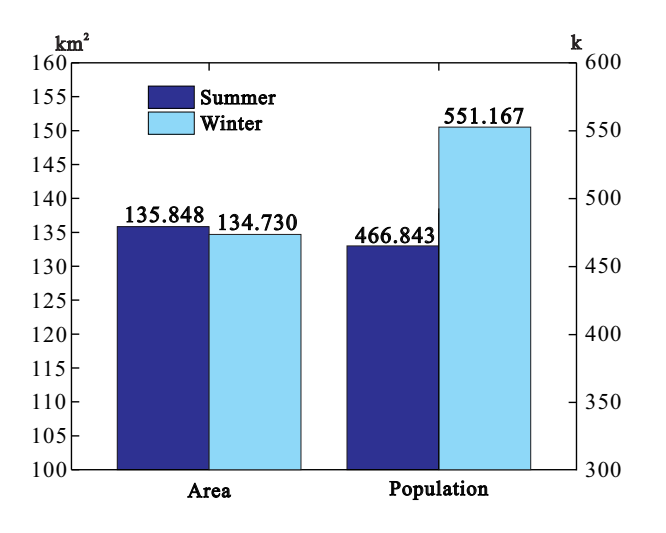


Figure 14: Noise-affected area and population of BIA in 2030 (Scenario 1) during summer and winter.

However, the noise-affected population during winter is 843,230 people more than that during summer. This is because the south aircraft noise contour during winter extends to the area with greater population density as shown in Figure 10(b) and Table A4.

4 Conclusions

The future aircraft noise-level prediction method using BIA as an example was proposed in this study. First, two future operation scenarios and future operation of BIA in 2030 were predicted based on the BIA existing operation data. Thereafter, the population of the nine administrative regions around BIA in 2030 were predicted based on the method from United Nations. Finally, the noise maps of BIAs under two different operation scenarios in 2030 during summer and winter were constructed. The noise exposure levels of BIA were evaluated based one the constructed noise maps.

The noise exposed area and population of BIA with noise level greater than 70 dB under Scenario 1 are less than those of Scenario 2 during both summer and winter. Most importantly, the noise exposed population of Scenario 2 during winter is much larger than that of Scenario 1 (9,837,800 more people). Thus, Scenario 1 is the operation scenario with lower aircraft noise pollution degree, and consequently, it is the recommenced operation scenario to be used in BIA in the future. In addition, the results showed that aircraft noise pollution degree of BIA will increase significantly in 2030, especially during winter where the noise exposed area and population when noise level is greater than 70 dB increase by 71.88 and 146.87% (Scenario 1), respectively, if compared to current data.

It can be concluded that the number and growth rate of noise exposed population in the future during winter are the highest. This is due to the difference of population density in the noise-affected area during the two seasons. Therefore, an airport should not only pay attention to the higher noise level caused by the airport development in the future, but an airport also needs to pay attention to the total noise exposed population around the airport. The results of this study can not only provide valuable information for BIA to maintain its sustainable development, but also provide a guidance for other large airports to predict future aircraft noise level. For future works, a systematic method should be developed to estimate the error (in \pm %) of the current noise prediction method so that the readers can roughly predict, for example, the highest and lowest possible noise levels of the particular location if future noise level of the location is 80 dB.

Funding information: This research was funded by Singapore Ministry of Education Academic Research Fund Tier 1 [R-265-000-639-114].

Author contributions: All authors have accepted responsibility for the entire content of this manuscript and consented to its submission to the journal, reviewed all the results and approved the final version of the manuscript. Conceptualization, HML & HPL; methodology, LZ; software, LZ; validation, LZ; formal analysis, LZ & JX; investigation, LZ; resources, HML & HPL; data curation, LZ; writing – original draft preparation, JX & HML; writing – review and editing, HML; visualization, LZ; supervision, JX; project administration, JX; funding acquisition, HPL.

Conflict of interest: The authors state no conflict of interest.

References

- World air passenger traffic evolution, 1980–2020. Energy Efficiency 2020; 2020. https://www.iea.org/data-and-statistics/charts/worldair-passenger-traffic-evolution-1980-2020.
- [2] Urban Development; 2020. https://www.worldbank.org/en/topic/ urbandevelopment/overview.
- [3] Aircraft noise effects on health. Queen Mary University of London; 2015.
- [4] Netjasov F. Contemporary measures for noise reduction in airport surroundings. Appl. Acoustics. 2012;73(10):1076–85.
- [5] Vogiatzis K. Airport environmental noise mapping and land use management as an environmental protection action policy tool. The case of the Larnaka International Airport (Cyprus). Sci. Total Environ. 2012;424:162–73.
- [6] Josimovic B, Krunic N, Nenkovic-Riznic M. The impact of airport noise as part of a strategic environmental assessment, case study.

- The Tivat (Montenegro) airport expansion plan. Transport Res Part D Transport Environ. 2016;49:271–9.
- [7] Ozkurt N. Current assessment and future projections of noise pollution at Ankara Esenboga Airport, Turkey Transport Res Part Dtransport Environ. 2014;32:120–8.
- [8] Sadr MK, Nassiri P, Hosseini M, Monavari M, Gharagozlou A. Assessment of land use compatibility and noise pollution at Imam Khomeini International Airport. | Air Transport Manag. 2014;34:49–56.
- [9] Wolfe PJ, Kramer JL, Barrett SRH. Current and future noise impacts of the UK hub airport. J Air Transport Manag. 2017;58:91–9.
- [10] Guangzhou Traffic Development Annual Report. Guangzhou Transportation Planning and Research Institute; 2020. http://www. gz.gov.cn/zt/ylctfjzx2019gzld/content/post-7722538.html.
- [11] Xie J, Zhu L, Lee HM. Novel methodologies for the development of large-scale airport noise map. Sustainability. 2022;14(11):6573.
- [12] Guangzhou Baiyun International Airport; 2022. https://en.wikipedia. org/wiki/GuangzhouBaiyunInternationalAirportcitenote3runway4.
- [13] Guangzhou Baiyun International Airport Phase III expansion project; 2020. http://www.gz.gov.cn/xw/gzyw/content/post-6729268.html.
- [14] Feasibility study report on phase III expansion project of Guangzhou Baiyun International Airport. China Airport Planning & Design Institute Co., Ltd.; 2020.

- [15] Guangzhou Baiyun International Airport Phase III Expansion
 Project Feasibility Study Report Receives Approval from National
 Development and Reform Commission; 2020. http://fgw.gz.gov.cn/fzgg/tzgl/content/post.html.
- [16] Order of the Civil Aviation Administration of China. Civil Aviation Administration of China; 2004. 123. http://www.gov.cn/gongbao/ content/2005/content63346.htm.
- [17] Arafa MH, Osman TA, Abdel-Latif IA. Noise assessment and mitigation schemes for Hurghada airport. Appl Acoustics. 2007;68(11–12):1373–85.
- [18] Population and distribution of resident in Guangzhou from 2010 to 2020. 2021. http://tjj.gz.gov.cn/tjgb/qtgb/content/post7912709.html.
- [19] Methods of Estimating Total Population for Current Dates. New York: United Nations; 1952. p. 10.
- [20] Bulletin of the seventh national census of Baiyun District, Guangzhou [1] (No. 2) – population of each town (street); 2021. http://www.by.gov.cn/ywdt/tzgg/content/post-7326984.html.
- [21] Bulletin of the seventh national census of Huadu District, Guangzhou [1] (No. 2) – population of each town (street); 2021. https://www.huadu.gov.cn/gkmlpt/content/7/7327/post-7327501.html.
- [22] Boya Place Name Sharing Site; 2022. http://www.tcmap.com.cn/guangdong/guangzhoushi.html.

Appendix

Table A1: Current aircraft takeoff tracks and the corresponding destinations in BIA during summer

Track	Direction relative to the airport	Destination			
T-19-A, T-19-B, T-20R-C	North, northwest, west	Harbin, Beijing, Changchun, Taiyuan, Tianjin, Chengdu, Chongqing, Lanzhou, Urumqi, Yichang, Zunyi, Nanyang, Zhangjiajie, Shijiazhuang, Nanchong, Wanzhou, Jingzhou, Yizhou, Yulin, Yuncheng, Sanxia, Tongren, Shenyang, Fuyang, Amsterdam, Liupanshui, Xi'an, Hohhot, Yinchuan, Yibin, Changde, Shijiazhuang, Wuhan, Jingzhou, Shiyan, Yuncheng, Bijie, Xichang, Mianyang, Zhengzhou, Fuyang, Hancheng, Xining, Yulin, Tongren, Longnan, Guiyang, Handan, Hanzhong, Jining, Anshan, Ankang, Taiyuan, Changsha, London, Luoyang,			
T-20R-A	Northeast, east, southeast	Guangyuan, Qianjiang, Frankfurt, Linzhi, <i>etc.</i> Jinan, Shanghai, Yantai, Dongying, Changzhou, Huangyan, Vancouver, Dalian, Quanzhou, Meizhou, Qingdao, Wenzhou, Fuzhou, Hefei, Taizhou, Meixian, Weihai, Weifang, Los Angeles, Dongying, San Francisco, New York, Xiamen, Zhoushan, Toronto, Anqing, Rizhao, Chizhou, Anchorage, Seoul, Nantong, Tokyo, Nanjing, Dhaka, Ningbo, Anqing, Obligation, Lianyungang, Nanchang, Yichun, Ganzhou, Jingdezhen, Ji'an, Yangzhou, Wuxi, Yancheng, Jieyang, Wuyishan, Fuzhou, Huaian, Huangshan, <i>etc.</i>			
T-20R-B, T-19-C	Nouthwest, south	Xingyi, Kunming, Dali, Jinghong, Sanya, Haikou, Baoshan, Phnom Penh, Manang, Zhanjiang, Auckland, Doha, Dhaka, Manila, Qionghai, Lijiang, Tengchong, Nanning, Islamabad, Wenshan, Shangri-La, Nebbiro, Kolkata, White, North Sea, Tehran, Taipei, Colombo, North Sea, Nanning, Dubai, Auckland, Doha, <i>etc</i> .			

Table A2: Current aircraft takeoff tracks and the corresponding destinations in BIA during winter

Track	Direction relative to the airport	Destination
T-01-A,	West, southwest, south	Anshan, Yichang, Lijiang, Linyi, Linzhi, Seoul, Colombo, Jinghong, Kunming, Xinyi, Sanya,
T-02L-A		Baoshan, Haikou, Beihai, Ethiopia, Dali, Kathmandu, Mangshi, Zhanjiang, Nairobi, Nanning, Dhaka, Phnom Penh, Diqing, Shangri-La, Ho Chi Minh City, Tehran, Bangkok, Auckland, Riyadh, Singapore, Zhanjiang, Nanning, Kuala Lumpur, Riyadh, <i>etc.</i>
T-01-B	Northwest	Shiyan, Chengdu, Chongqing, Xi'an, Nanchong, Dazhou, Yibin, Yinchuan, Wanzhou, Luzhou, Zunyi, Shaotong, Guiyang, Ankang, Yulin, Tongren, Longnan, Mianyang, Urumqi, Wushan, Frankfurt, Bijie, Bishkek, Xi'an, Lanzhou, Guiyang, Bijie, Mianyang, Atatürk, <i>etc</i> .
T-01-C,	North	Yichang, Sanxia, Luoyang, Shijiazhuang, Lanzhou, Harbin, Wuhan, Changsha, Xiangyang,
T-02L-B		Yuncheng, Luzhou, Hohhot, Taiyuan, Shenyang, Yizhou, Bishkek, Linyi, Taiyuan, Changde, Tianjin, Anshan, Nanyang, Changchun, Nanyang, Beijing, Jining, Zhengzhou, Qinhuangdao, Xinyang, Tangshan, Zhangjiajie, Fuyang, Urumqi, Handan, Tianjin, Yuncheng, Almaty, <i>etc</i> .
T-02L-C	Northeast, east, southeast	Jinan, Shanghai, Yantai, Dongying, Changzhou, Huangyan, Vancouver, Dalian, Quanzhou, Meizhou, Qingdao, Wenzhou, Fuzhou, Hefei, Taizhou, Meixian, Weihai, Weifang, Los Angeles, Dongying, San Francisco, New York, Xiamen, Zhoushan, Toronto, Anqing, Rizhao, Chizhou, Anchorage, Seoul, Nantong, Tokyo, Nanjing, Dhaka, Ningbo, Anqing, Obligation, Lianyungang, Nanchang, Yichun, Ganzhou, Jingdezhen, Ji'an, Yangzhou, Wuxi, Yancheng, Jieyang, Wuyishan, Fuzhou, Huaian, Huangshan, <i>etc</i> .

Table A3: Operation mode of parallel runway [16]

Spacing	Mode	Operation
<760 m	Release single runway with time interval	One runway is only used for landing, and another runway is only used for takeoff based on the specified time interval
≥760 m	Segregated parallel approach/ departure	One runway is only used for departure, and another runway is only used for approach
≥760 m	Independent parallel departure	Simultaneous takeoffs on the parallel runways are possible if the flying directions of the aircrafts are the same
≥915 m	Dependent parallel approach	Simultaneous landings on the parallel runways are possible if the specified spacing between the two aircrafts is complied
≥1,035 m	Independent parallel approach	Simultaneous landings on the parallel runways are possible if the specified spacing between the two aircrafts is not complied.

Table A4: Population densities of the nine administrative regions around BIA in 2030

Region	Direction relative to the airport	Area (km²)	Population	Population density (people/km²)
Huadong town	North	208.44	250,414	2519
Huashan town	Northwest	116	174,842	839
Xinya street	Southwest	32.98	244,492	7413
Renhe town	South	74.15	292,114	3,940
Longgui street	South	26.71	269,336	10,084
Taihe town	Southeast	155.37	182,243	1173
Junhe street	South	19.8	238,056	12,023
Jiahe street	South	9.8	242,557	24,751
Zhongluotan town	East	169.4	380,450	2,246

The area of each region can be found from [22].